

## Catalytic Foldamers

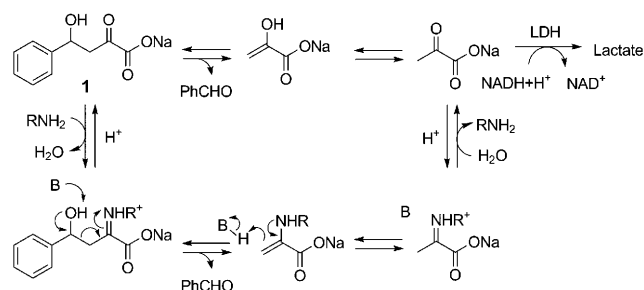
## A Rationally Designed Aldolase Foldamer\*\*

Manuel M. Müller, Matthew A. Windsor, William C. Pomerantz, Samuel H. Gellman,\* and Donald Hilvert\*

Current strategies for creating enzyme-like catalysts range from rational<sup>[1]</sup> and computational design<sup>[2]</sup> to evolutionary searches of large molecular libraries.<sup>[3]</sup> Sequence-specific polymers are particularly attractive starting points for these approaches because of their ability to adopt three-dimensional structures that preorganize functional groups for catalysis. Although natural enzymes are constructed from  $\alpha$ -amino acids, many other backbone structures can give rise to well-defined secondary and tertiary structures. Such non-natural oligomers, often referred to as “foldamers”, have the potential to display properties akin to those of proteins.<sup>[4–8]</sup>

$\beta$ -Peptides are interesting in this context because they adopt a variety of stable secondary structures, including helices, sheets, and turns,<sup>[4,9]</sup> quaternary helix-bundle assemblies have also been generated.<sup>[10,11]</sup> Their predictable structures have been exploited to inhibit microbial growth,<sup>[12]</sup> disrupt protein–protein interactions,<sup>[13]</sup> and for other applications.<sup>[4,5]</sup> Herein we report that  $\beta$ -peptides presenting arrays of discrete side-chain functional groups can also act as effective catalysts.

As a model reaction, we examined the retroaldol cleavage of  $\beta$ -hydroxyketone **1** to give benzaldehyde and pyruvate. This reaction is subject to amine catalysis (Scheme 1). The catalytic cycle is initiated by nucleophilic attack of an amine on the carbonyl group of the substrate. The resulting iminium ion activates the substrate for C–C bond scission, which occurs with concomitant deprotonation of the hydroxyl group to release benzaldehyde. Tautomerization of the enamine and subsequent hydrolysis produces pyruvate and regenerates the catalyst. This mechanism is exploited by natural type-I aldolases,<sup>[14]</sup> and has been mimicked by lysine-rich amphiphilic  $\alpha$ -helical peptides,<sup>[15]</sup> catalytic antibodies,<sup>[16]</sup> and most recently by a computationally designed enzyme.<sup>[2a]</sup>



**Scheme 1.** Retroaldol reaction of sodium 4-phenyl-4-hydroxy-2-oxobutyrate (**1**) and the mechanism of amine catalysis.

Since imine formation is partially limiting in an aqueous environment,<sup>[17]</sup> the challenge in the design of catalysts for such retroaldol reactions is to provide a nucleophilic amine under physiological conditions. Studies of enzymes that exploit imine or enamine formation have shown that amine nucleophilicity can be significantly enhanced through coulombic interactions with nearby cations, which increase the population of the unprotonated state.<sup>[18]</sup> This strategy, which has been successfully utilized in the design of helical  $\alpha$ -peptide catalysts,<sup>[15,17,19]</sup> can be extended to the construction of helical  $\beta$ -peptide catalysts.

One of the best-understood  $\beta$ -peptide secondary structures is the 14-helix, which is characterized by 14-membered ring hydrogen bonds between the N–H unit of residue  $i$  and C=O unit of residue  $i + 2$ .<sup>[4,9]</sup> This helix is favored by  $\beta^3$ -amino acid residues, which bear a side chain on the backbone carbon atom adjacent to the nitrogen atom. To stabilize such structures in aqueous solution, electrostatic interactions between the side chains<sup>[20]</sup> or conformationally restricted building blocks<sup>[21]</sup> can be employed. For example, the cyclically constrained *trans*-2-aminocyclohexanecarboxylic acid (ACHC), which has a very high propensity to adopt a helical conformation, has been used to construct short  $\beta$ -peptides that reliably adopt the 14-helical conformation in water, regardless of temperature, pH, or concentration.<sup>[21,22]</sup> A  $\beta$ -peptide sequence that contains multiple ACHC residues along with  $\beta^3$ -homolysine ( $\beta^3$ -hLys) residues in an  $i, i + 3, i + 6$  array should lead to alignment of the amine-containing side chains along one side of a 14-helix (Scheme 2). We anticipated that this clustering of  $\beta^3$ -hLys residues would cause a decrease in side-chain ammonium  $pK_a$  values and thus facilitate amine catalysis of the retroaldol reaction of **1**.

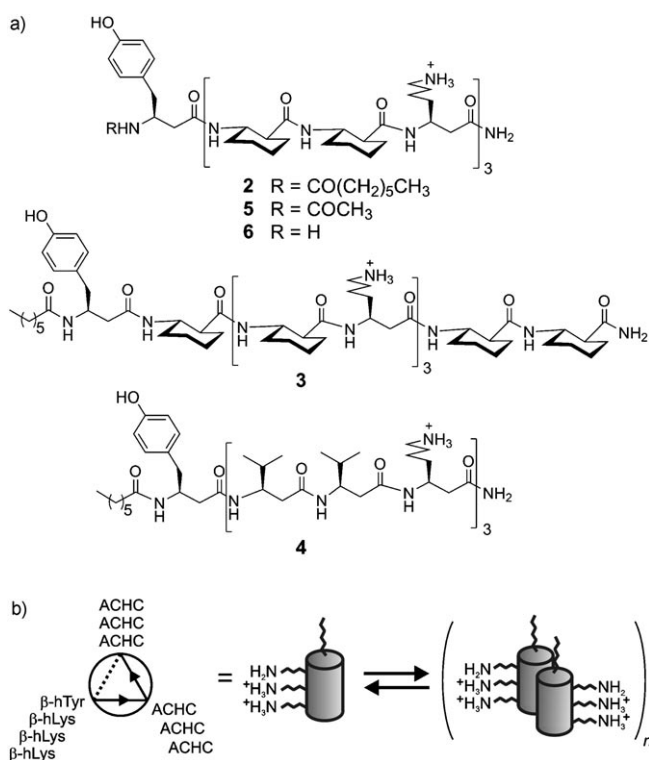
Our design hypothesis was tested with  $\beta$ -peptides **2–4** (Scheme 2).  $\beta$ -Peptide **2** has three ACHC-ACHC- $\beta^3$ -hLys triad repeats, a  $\beta^3$ -hTyr residue to facilitate concentration determination, and an N terminus that is capped with a heptanoyl moiety to promote self-assembly.<sup>[23]</sup> Isomeric  $\beta$ -

[\*] M. A. Windsor, Dr. W. C. Pomerantz, Prof. Dr. S. H. Gellman  
Department of Chemistry, University of Wisconsin-Madison  
1101 University Avenue, Madison, WI 53706 (USA)  
Fax: (+1) 608-265-4534  
E-mail: gellman@chem.wisc.edu

M. M. Müller, Prof. Dr. D. Hilvert  
Laboratorium für Organische Chemie, ETH Zürich  
Hönggerberg HCI F339, 8093 Zürich (Switzerland)  
Fax: (+41) 44-632-1486  
E-mail: hilvert@org.chem.ethz.ch

[\*\*] This work was supported by the Schweizerischer Nationalfonds, NIH grant GM056414 (to S.H.G.), and the Nanoscale Science and Engineering Center at UW-Madison (NSF DMR-042588). We thank Dr. Dennis Gillingham for help with substrate preparation.

Supporting information for this article is available on the WWW under <http://dx.doi.org/10.1002/anie.200804996>.



**Scheme 2.** a) Sequences of  $\beta$ -peptides 2–6. b) Helical wheel diagram of  $\beta$ -peptide 2 (left) and a cartoon showing  $\beta$ -peptide self-assembly (right; the partial protonation state shown is purely hypothetical).

peptide **3** has a scrambled sequence that does not match the three-residue repeat of the 14-helix; the three  $\beta^3$ -hLys residues of **3** should therefore be dispersed around the 14-helix periphery rather than held in close alignment, as in **2**. Comparison of the activities of **2** and **3** allows us to determine whether the spatial arrangement of the  $\beta^3$ -hLys residues is important for catalysis.  $\beta$ -Peptide **4** is an analogue of **2** in which all of the preorganized ACHC residues are replaced by flexible  $\beta^3$ -hVal residues. Comparison of the activities of **4** and **2** allows us to assess the importance of helical folding for catalysis.

Circular dichroism (CD) measurements provided preliminary insight into the folding and self-assembly of  $\beta$ -peptides **2–4**; although CD is an intrinsically low-resolution method, previous correlations with 2D NMR spectroscopy and analytical ultracentrifugation (AU) data provide a basis for interpretation.<sup>[22]</sup> CD data indicate that **2** is highly 14-helical and self-assembled in aqueous buffer, that **3** is comparably folded but not self-assembled,<sup>[22]</sup> and that **4** is largely unfolded (Figure S1 in the Supporting Information). The dramatic conformational difference between **2** and **3**, which contain ACHC residues, and **4**, which lacks ACHC residues, highlights the strong 14-helix stabilization provided by preorganization at the residue level. Further characterization by NMR spectroscopy (**2–4**) and AU (**2**) supports the conclusion that **2** forms large assemblies, while **3** and **4** undergo relatively little self-association (Figure S2 in the Supporting Information). The observation that **2** avidly self-associates, while **3** and **4** do not, indicates that the heptanoyl unit alone is insufficient to induce self-association. Instead, there appears to be a cooperative effect from pairing this terminal unit with a  $\beta$ -peptide segment that forms a stable helical conformation and displays a large, uninterrupted hydrophobic surface. Comparable cooperative effects have been observed among terminally modified  $\alpha$ -peptides.<sup>[23]</sup>

The  $\beta$ -peptides were tested for their ability to promote the retroaldol cleavage of **1**, an anionic substrate that is expected to bind well to the cationic catalysts. The reaction was monitored by a standard coupled assay in which lactate dehydrogenase (LDH) was used to catalyze the reduction of pyruvate (a retroaldol product) by NADH (NADH = reduced nicotinamide adenine dinucleotide).  $\beta$ -Peptide **2** promotes the retroaldol cleavage of **1** with multiple turnovers (Figure S3 in the Supporting Information) and significant rate accelerations over the uncatalyzed reaction. In contrast,  $\beta$ -peptides **3** and **4** are relatively poor catalysts under identical conditions (Figure 1 a). The 20- to 50-fold lower activity for these control  $\beta$ -peptides shows that the activity of **2** requires both a well-folded helix and a properly arrayed set of  $\beta^3$ -hLys side chains.

The impact of N-terminal acyl group modification indicates that  $\beta$ -peptide self-assembly is important for generation

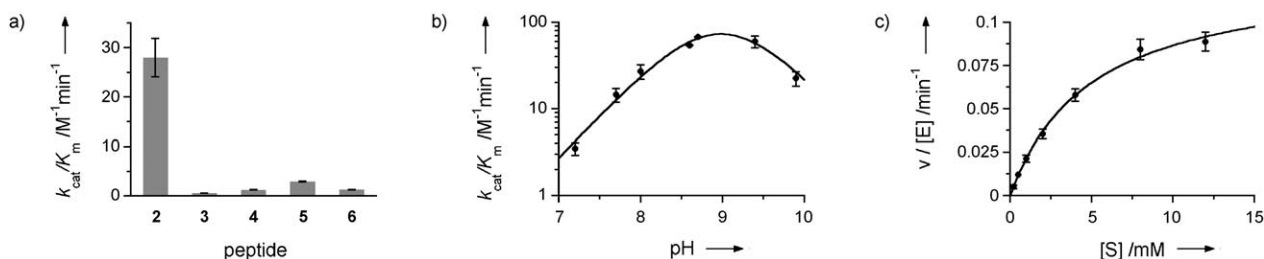


**Figure 1.** Kinetic characterization of  $\beta$ -peptide aldolases. Retroaldol reactions were performed in quartz cuvettes with  $\beta$ -peptide (50  $\mu\text{M}$ ), substrate **1** (0.5 mM), NADH (0.1 mM), and LDH (1 U mL<sup>-1</sup>) in tris(hydroxymethyl)aminomethane hydrochloride (tris-HCl, 50 mM, pH 8) containing NaCl (150 mM), at 30°C. Product formation was coupled to the oxidation of NADH through the LDH-catalyzed reduction of pyruvate and monitored spectroscopically at 340 nm ( $\epsilon_{\text{NADH}} = 6220 \text{ M}^{-1} \text{ cm}^{-1}$ ). Rates were corrected for background retroaldol cleavage and elimination reactions.

a) Specific activities of  $\beta$ -peptides 2–6. b) pH rate profile for  $\beta$ -peptide **2**. Additional LDH (10 U mL<sup>-1</sup>) was added to compensate for the reduced dehydrogenase activity at high pH values. The rate profile was fitted to the equation  $k_{\text{cat}}/K_m = k_{\text{HA}} / (1 + 10^{\text{pK}_{\text{a1}} - \text{pH}} + 10^{\text{pH} - \text{pK}_{\text{a2}}})$ . c) Michaelis–Menten plot for **2**. The dependence of rate on substrate concentration was determined both in continuous and discontinuous assay formats. Reactions were performed in Tris-HCl (50 mM, pH 8) containing NaCl (150 mM),  $\beta$ -peptide **2** (50  $\mu\text{M}$ ), and substrate (0.2–12 mM) at 30°C. NADH (0.5 mM) and LDH (2 U mL<sup>-1</sup>) were added for continuous monitoring.

of the catalytic species. Replacement of the heptanoyl group with an acetyl group to generate  $\beta$ -peptide **5** reduces the characteristic CD signature for self-assembly, but not the CD signature for 14-helical secondary structure (Figure S1 in the Supporting Information); the catalytic activity of **5** is an order of magnitude less than that of **2**.  $\beta$ -Peptide **6**, which lacks the acyl group altogether, is monomeric up to a concentration of approximately 1 mM,<sup>[10a]</sup> and is more than 20-times less active than **2**. Some  $\alpha$ -peptides designed for amine-mediated catalysis benefit from self-assembly;<sup>[17]</sup> the interpeptide interactions in these systems lead to a significant enhancement of  $\alpha$ -helical folding. In contrast, the benefit of self-assembly for  $\beta$ -peptide catalysis is unlikely to be caused by an increase in 14-helicity, because ACHC-rich sequences such as those of **2**, **3**, **5**, and **6** afford very high populations of the helical conformation in aqueous solution even when the  $\beta$ -peptides remain monomeric.<sup>[21,22]</sup> The favorable effects that arise from the clustering of  $\beta$ -peptide molecules may reflect a further reduction in the  $pK_a$  value of the  $\beta^3$ -hLys side-chain ammonium group, which occurs as a result of high local positive-charge density or an increase in the hydrophobicity of the environment of catalytic amines. Alternatively, an interface between helical  $\beta$ -peptides could act as a primitive substrate-binding pocket. These postulated effects could operate in tandem.

As suggested by the mechanism proposed in Scheme 1, the reaction catalyzed by **2** is pH-dependent. A bell-shaped pH rate profile is observed, with a maximum rate at pH 9 and  $pK_1 = (8.8 \pm 0.2)$  and  $pK_2 = (9.2 \pm 0.2)$  (Figure 1b). Although the available data do not allow assignment of the inflections to specific ionizing groups, the lower value is consistent with the participation of a  $\beta^3$ -hLys side-chain amino group that has an unusually low  $pK_a$  value. The decrease in activity at high pH value could indicate bifunctional acid–base catalysis, or reflect a change in the aggregation state of the  $\beta$ -peptide. Additional evidence for the postulated mechanism was obtained by trapping imine intermediates by reduction with NaCNBH<sub>3</sub>. Signals that correspond to peptides modified with pyruvate product, one or two aldol substrates, and one aldol plus one pyruvate group were detected by LC–MS (Figure S4 in the Supporting Information).

The efficiency of  $\beta$ -peptide catalysis was evaluated by using steady-state kinetic measurements. The retroaldolase reaction catalyzed by **2** follows Michaelis–Menten behavior (Figure 1c). At pH 8.0 and 30 °C, the steady-state parameters  $k_{cat}$  and  $K_m$  are  $(0.13 \pm 0.01) \text{ min}^{-1}$  and  $(5.0 \pm 0.6) \text{ mM}$ , respectively. Comparison of the turnover number with the rate constant for the uncatalyzed retroaldol reaction under identical conditions (Figure S5 in the Supporting Information) gives a rate acceleration of  $k_{cat}/k_{uncat} = 3000$ . Although substantially lower than the rate accelerations achieved by natural enzymes, this value compares favorably with the activity of catalysts designed for the cleavage of 4-hydroxy-4-(6-methoxy-2-naphthyl)-2-butanone, a process related to the retroaldol reaction of **1**. Thus, the simple  $\beta$ -peptide **2** is roughly twice as efficient as evolutionarily optimized  $\alpha$ -peptide aldolases ( $k_{cat} = 5.6 \times 10^{-4} \text{ min}^{-1}$ ,  $K_m = 1.8 \text{ mM}$ , and  $k_{cat}/k_{uncat} = 1400$ ),<sup>[15]</sup> and only eight times less efficient than the best computationally designed aldolases ( $k_{cat} = 9.6 \times$

$10^{-3} \text{ min}^{-1}$ ,  $K_m = 0.5 \text{ mM}$ ,  $k_{cat}/k_{uncat} = 24000$ ).<sup>[2a]</sup> The small difference in rate enhancement between a 10-residue  $\beta$ -peptide and a 200-residue protein underscores the catalytic potential in  $\beta$ -peptide scaffolds. Furthermore, unlike helices formed by  $\alpha$ -peptides, the  $\beta$ -peptide 14-helix is very stable when preorganized ACHC residues are incorporated into it. In fact,  $\beta$ -peptide **2** retains high aldolase activity even at 80 °C ( $k_{cat} = (3.5 \pm 0.2) \text{ min}^{-1}$ ,  $K_m = (5.5 \pm 1.0) \text{ mM}$ ,  $k_{cat}/k_{uncat} = 1300$ ; Figure S6 and S7 in the Supporting Information), which firmly illustrates the robust nature of this scaffold.

Although only 10 residues long and designed according to very simple principles,  $\beta$ -peptide **2** displays excellent catalytic properties. Our results suggest that  $\beta$ -peptidic structures may be versatile scaffolds for engineering catalytic activities. Nevertheless, the prototypic  $\beta$ -peptide catalyst presented here is not optimal. The high  $K_m$  value likely reflects the lack of a defined substrate-binding pocket. The change from a secondary to a tertiary structure should allow creation of true active sites in which functional groups can be effectively oriented for highly efficient catalysis. Recent approaches toward higher-order foldamer structures,<sup>[8,11,24]</sup> and the diversity of backbone chemistry available to folding oligomers in general,<sup>[5,6]</sup> present exciting opportunities for the development of more sophisticated catalysts.

Received: October 13, 2008

Revised: November 11, 2008

Published online: December 18, 2008

**Keywords:** aldol reaction · enzyme models · homogeneous catalysis · peptides · preorganization

- [1] R. Breslow, *Artificial Enzymes*, Wiley-VCH, Weinheim, **2005**.
- [2] a) L. Jiang, E. A. Althoff, F. R. Clemente, L. Doyle, D. Röthlisberger, A. Zanghellini, J. L. Gallaher, J. L. Betker, F. Tanaka, C. F. Barbas III, D. Hilvert, K. N. Houk, B. L. Stoddard, D. Baker, *Science* **2008**, *319*, 1387–1391; b) D. Röthlisberger, O. Khersonsky, A. M. Wollacott, L. Jiang, J. DeChance, J. Betker, J. L. Gallaher, E. A. Althoff, A. Zanghellini, O. Dym, S. Albeck, K. N. Houk, D. S. Tawfik, D. Baker, *Nature* **2008**, *453*, 190–195.
- [3] a) C. Jäckel, P. Kast, D. Hilvert, *Annu. Rev. Biophys.* **2008**, *37*, 153–173; b) S. J. Miller, *Acc. Chem. Res.* **2004**, *37*, 601–610.
- [4] D. Seebach, A. K. Beck, D. J. Bierbaum, *Chem. Biodiversity* **2004**, *1*, 1111–1239.
- [5] C. M. Goodman, S. Choi, S. Shandler, W. F. DeGrado, *Nat. Chem. Biol.* **2007**, *3*, 252–262.
- [6] S. Hecht, I. Huc, *Foldamers: Structure, Properties, and Applications*, Wiley-VCH, Weinheim, **2007**.
- [7] See for example: a) R. A. Smaldone, J. S. Moore, *Chem. Eur. J.* **2008**, *14*, 2650–2657; b) H. P. Yi, J. Wu, K. L. Ding, X. K. Jiang, Z. T. Li, *J. Org. Chem.* **2007**, *72*, 870–877.
- [8] B.-C. Lee, T. K. Chu, K. A. Dill, R. N. Zuckermann, *J. Am. Chem. Soc.* **2008**, *130*, 8847–8855.
- [9] R. P. Cheng, S. H. Gellman, W. F. DeGrado, *Chem. Rev.* **2001**, *101*, 3219–3232.
- [10] a) T. L. Raguse, J. R. Lai, P. R. LePlae, S. H. Gellman, *Org. Lett.* **2001**, *3*, 3963–3966; b) R. P. Cheng, W. F. DeGrado, *J. Am. Chem. Soc.* **2002**, *124*, 11564–11565.
- [11] D. S. Daniels, E. J. Petersson, J. X. Qiu, A. Schepartz, *J. Am. Chem. Soc.* **2007**, *129*, 1532–1533.

- [12] a) E. A. Porter, X. Wang, H.-S. Lee, B. Weisblum, S. H. Gellman, *Nature* **2000**, *404*, 565–565; b) D. Liu, W. F. DeGrado, *J. Am. Chem. Soc.* **2001**, *123*, 7553–7559; c) P. I. Arvidsson, N. S. Ryder, H. M. Weiss, G. Gross, O. Kretz, R. Woessner, D. Seebach, *ChemBioChem* **2003**, *4*, 1345–1347.
- [13] a) M. Werder, H. Hauser, S. Abele, D. Seebach, *Helv. Chim. Acta* **1999**, *82*, 1774–1783; b) J. A. Kritzer, N. W. Luedtke, E. A. Harker, A. Schepartz, *J. Am. Chem. Soc.* **2005**, *127*, 14584–14585; c) E. P. English, R. S. Chumanov, S. H. Gellman, T. Compton, *J. Biol. Chem.* **2006**, *281*, 2661–2667.
- [14] A. Heine, G. DeSantis, J. G. Luz, M. Mitchell, C.-H. Wong, I. A. Wilson, *Science* **2001**, *294*, 369–374.
- [15] F. Tanaka, R. Fuller, C. F. Barbas III, *Biochemistry* **2005**, *44*, 7583–7592.
- [16] J. Wagner, R. A. Lerner, C. F. Barbas III, *Science* **1995**, *270*, 1797–1800.
- [17] K. Johnsson, R. K. Allemann, H. Widmer, S. A. Benner, *Nature* **1993**, *365*, 530–532.
- [18] F. H. Westheimer, *Tetrahedron* **1995**, *51*, 3–20.
- [19] C. J. Weston, C. H. Cureton, M. J. Calvert, O. S. Smart, R. K. Allemann, *ChemBioChem* **2004**, *5*, 1075–1080.
- [20] a) R. P. Cheng, W. F. DeGrado, *J. Am. Chem. Soc.* **2001**, *123*, 5162–5163; b) P. I. Arvidsson, M. Rueping, D. Seebach, *Chem. Commun.* **2001**, 649–650.
- [21] T. L. Raguse, J. R. Lai, S. H. Gellman, *J. Am. Chem. Soc.* **2003**, *125*, 5592–5593.
- [22] a) W. C. Pomerantz, T. L. R. Grygiel, J. R. Lai, S. H. Gellman, *Org. Lett.* **2008**, *10*, 1799–1802; b) E. Vaz, W. C. Pomerantz, M. M. Geyer, S. H. Gellman, L. Brunsveld, *ChemBioChem* **2008**, *9*, 2254–2259.
- [23] a) Y. C. Yu, M. Tirrell, G. B. Fields, *J. Am. Chem. Soc.* **1998**, *120*, 9979–9987; b) D. L. Daugherty, S. H. Gellman, *J. Am. Chem. Soc.* **1999**, *121*, 4325–4333.
- [24] W. S. Horne, J. L. Price, S. H. Gellman, *Proc. Natl. Acad. Sci. USA* **2008**, *105*, 9151–9156.